Numerical Modelling for Optimization of Fibres Winding Process of Manufacturing Technology for the Non-Circular Aerospaces Frames

Michal Petru, Jaroslav Mlynek, Tomas Martinec
Technical University of Liberec, Studentská 2, 461 17, Liberec 1, Czech Republic. E-mail: michal.petru@tul.cz, tomas.martinec@tul.cz, jaroslav.mlynek@tul.cz

This article deals with the issue of mathematical calculating the trajectory of the end-effector of an industrial robot in the manufacture of aerospace composites. Robots are used to define the winding orientation of the fibre strands on a non-bearing 3D core. The 3D core is attached to the robot-end-effector and is led through a fibre-processing head according to a suitably defined robot trajectory during winding of the fibre on the core. The quality of the composite depends greatly on the correct winding angles of the fibres on the frame and on the homogeneity of the individual winding layers. The implementation of these two conditions is related to determining the correct trajectory of the industrial robot, which is part of the composite production technology. The numerical modelling of a passage of the on-bearing 3D core through a fibre-processing head is described in the article. Differential evolution algorithm and matrix calculus are applied to the numerical calculation of optimized robot-end-effector trajectory to achieve optimal angles of windings of fibres on the frame. The numerical calculations of the trajectory of the robot-end-effector were used for verified for the calculated trajectory of the robot-end-effector in the real conditions of robotic laboratory of department of machinery construction.

Keywords: Numerical modelling, Optimization, Aerospace frame, Composite materials, Winding technology.

1 Introduction

Currently, traditional materials are very often replaced by composite materials in many industrial areas. The advantages of these materials consist mainly in their lightweight, high strength and flexibility, corrosion resistance and a long lifespan. The use of composites reaches its large development in the field of aerospace. This article deals with the production process of a specific composite type for aerospace industry. We describe the technology of a organic / anorganic filament roving winding on a non-bearing frame in 3D with circular cross-section (i.e. see [1,2]. If the frame cross-section is not circular, we consider an imaginary cylindrical "envelope" (with minimum possible radius) stretched on the frame surface. The composites offer an attractive ratio of material properties-to-production costs (for example see [3,4,5]. Traditional procedures of composite manufacturing are labour-intensive and time-consuming. Moreover, the conventional techniques do not ensure accurate fiber winding on the frame. One of the possible approaches to producing composites is to stretch the fabric from the fibres on a frame with an arbitrary geometry. However, if the frame of the composite is a closed 3D frame or a frame with a very complicated 3D shape or several layers of the fiber strands are wound simultaneously on the frame, then this approach is not suitable. In such cases, the method of winding of endless fibre strands on a frame geometry using rotary fibre-processing head is often used [1,2]. The use of industrial robots in composite production greatly reduces production costs, production time and minimizes scrap rate (see [6,7,8]). This method provides full control over the placement, laying direction, and the amount of fibres on the frame as well as the homogeneity of the structure. The final composite is obtained after dry winding of the required layers of strands on the frame by injection of the resin to the mould using heat and pressure.

Now, we describe the manufacturing process for producing composites with non-bearing frame by method of dry winding on a frame. We tested this manufacturing process at our experimental robotic laboratory of department of machinery construction at Technical university of Liberec. The key equipment of our laboratory is an industry robot KR 16-2 and fibre-processing head. The fibre-processing head is fixed in the workspace of the robot and coordinates of its parts are specified in the basic coordinate system of the robot. The used fibre-processing head contains three guidelines. Each guideline contains twelve fixed fibre coils along its periphery. The outer guidelines rotate around a common axis and the intermediate guideline is static.The frame is attached to the end-effector of the robot. The passage of the frame through the fibre-processing head is controlled by the movement of the robot-end-effector. When frame passes through fibre-processing head the strands are successively wound on the surface of the frame at a targeted angle. First the outer rotating guideline ensures winding strands under the 30°,45°,60° angle (relative to the axis of the head and the moving direction of the frame). Subsequently, the middle static guideline winds the second layer of strand under the angle of 0° and the second outer guideline winds the final layer of strands at -30°,-45°,-60°. Our goal is that the frame passes through the fibre-processing head orthogonally to the guidelines of the head as far as possible. This ensures right angles of the individual winding layers. As already mentioned [2], providing the correct winding angles of strands on the frame is mainly conditioned upon the determination of the finding of the appropriate trajectory of the robot-end-effector. The orthogonal direction of passage of the frame to the guideline in the place of its owns fiber winding on frame surface ensures the correct angle and uniformity of winding. The quality of fiber windings also depends on the preserving of the proper ratio of the passage speed of the frame through the winding head and the angular rotation speed of the guide line. The material properties of the non-bearing 3D frame and fibers also affect the quality of the fiber windings (especially on adhesion of fiber to the frame), see e.g [9,10]. The problems concerning industrial robot trajectories are solved in more articles. Procedures of manual determining the robot trajectory through the teach pendant are described for example in article [11]. The optimization of the robot trajectory in terms of time is solved for example in article [12].

2 Optimization of fibres winding process of manufacturing technology for the non-circular aerospaces frames

This chapter describes the mathematical model of the manufacturing process of fibres winding on the frame. It is a similar principle to [2], the difference being that it is a non-circular cross-section of the closed frame.The actual process of winding is realized using a fibre-processing head and industrial robot. The non-bearing frame is attached to the robot-end-effector. The winding head is fixed in the workspace of the robot. Within the described numerical model, we will consider the right-handed Euclidean coordinate system E_3 of the robot (*BCS*). We will describe the positions of the individual parts of an experimental workplace of winding strands to frame using this coordinate system.

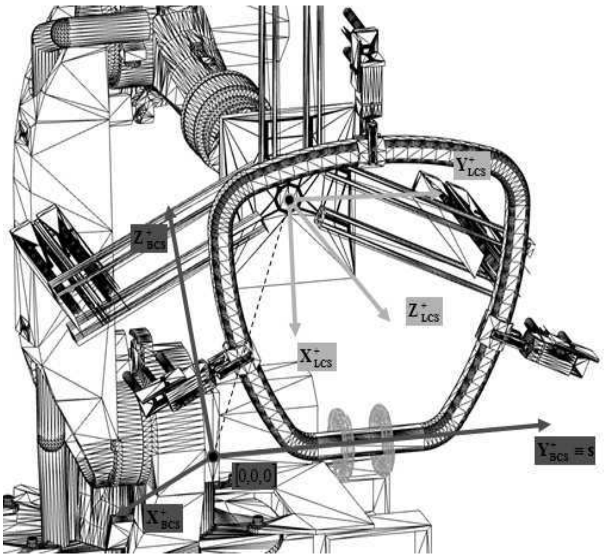

***Fig. 1** Numerical model for optimization of fibres winding process of manufacturing technology for the aerospaces frames*

The non-bearing frame with non-circular cross-section is attached to the REE. In the numerical model (Fig.1), robot workspace is defined by the base right-handed Euclidean coordinate system E_3 (*BCS*). Description ofthe location of individual subjects in robot workspace is made in *BCS*. Subsequently, we determine the local right-handed Euclidean coordinate system E_3 (*LCS*). This system describes location and orientation of REE towards *BCS*. In the following text, we will label the vectors and points with coordinates in *BCS* with the subscript $_{BCS}$ and vectors and points with coordinates in *LCS* with the subscript $_{LCS}$. All working activities of an industrial robot are controlled by the robot central unit and the library of instructions through REE. The location and orientation of REE is defined by *LCS*. The *LCS* origin is positioned in the REE while at the same time the REE is oriented in the direction of the positive part of the *z*-axis in the *LCS* with regard to the *BCS*. The actual location of the *LCS* with regard to the *BCS* is determined by six parameters listed in the tool-centre-point (*TCP*), where *TCP* = (*x*, *y*, *z*, *a*, *b*, *c*). The first three values specify the coordinates of the origin of the *LCS* in regard to the *BCS*. The last three values *a*, *b* and *c* specify the angle of the rotation of the *LCS* around axes *z*, *y*, and *x* with regard to the *BCS*. The fibre-processing head is fixedly located in the working space of the robot. In our numerical model, individual components of the head are described by coordinates in *BCS*. The first outer rotating guide line is presented by circle $k1$ with the centre $S1_{BCS} = [x_{S1}, y_{S1}, z_{S1}]_{BCS}$ (see ***Fig.2***). The second outer rotating guide line is presented by circle $k2$ with the centre $S2_{BCS} = [x_{S2}, y_{S2}, z_{S2}]_{BCS}$. The static middle guide line (enables the placement of the fibres in a longitudinal direction) need not considered in the model. The circle $k1$ and $k2$ have the same radius r_{CIRCLE} . Centres $S1_{BCS}$ and $S2_{BCS}$ lie on axis *s* of the fibre-processing head. The centre of the head is represented by point H_{BCS} that lies in the middle of segment $S1_{BCS}S2_{BCS}$. Unit vector $\mathbf{h1}_{BCS}$ (this vector indicates the direction of passage frame through the head; usually $\mathbf{h1}_{BCS}$ $=(S2_{BCS}-S1_{BCS})/\|S2_{BCS}-S1_{BCS}\|$, where $\|S2_{BCS}-S1_{BCS}\|$ is the length of segment $S1_{BCS}S2_{BCS}$) and vector $\mathbf{h2}_{BCS}$ are defined, vectors $\mathbf{h1}_{BCS}$ and $\mathbf{h2}_{BCS}$ are orthogonal ($\mathbf{h1}_{BCS} \perp \mathbf{h2}_{BCS}$). Point H_{BCS} together with defined vectors $\mathbf{h1}_{BCS}$ and $\mathbf{h2}_{BCS}$ allow us to calculate a suitable trajectory of REE when the frame passes through the head. We suppose the non-bearing frame has a non-circular cross-section. Then the frame can be described by its central axis o and radius $\mathbf{r}_{TUBE}$, we suppose that $r_{\mathrm{CIRCLE}} > r_{FRAME}$ Sizes of frame are defined in *LCS* of the REE. From starting point $B(1)_{LCS}$ to endpoint $B(N)_{LCS}$ is marked *d*. At the same time, unit tangent vector $\mathbf{b1}(i)_{LCS}$ to axis o at point $B(i)_{LCS}$ is entered for $1 \le i \le N$. In addition, unit vector $\mathbf{b2}(i)_{LCS}$ is defined ($1 \le i \le N$) which when passing point $B(i)_{LCS}$ through the fibre-processing characterizes the necessary rotation of the frame about axis o. All the time $\mathbf{b1}(i)_{LCS} \perp \mathbf{b2}(\mathrm{i})_{LCS}$ holds. We assume that the discrete set of points $B(i)_{LCS}$ specifies axis o sufficiently densely and defines with a sufficient accuracy the shape of the frame. If frame is closed, the initial point of axis o is identical to endpoint (i.e. $B(1)_{LCS} \equiv B(N)_{LCS}$, $\mathbf{b1}(1)_{LCS} \equiv \mathbf{b1}(N)_{LCS}$ and $\mathbf{b2}(1)_{LCS} \equiv \mathrm{b}\mathbf{2}(N)_{LCS}$).

2.1 Calculation of the trajectory

Background of calculation

We describe the main idea of calculating the REE trajectory in this chapter. Note that the frame is fixed to the REE. The goal is to calculate the REE trajectory that ensures a gradual passage of axis *o* through the centre H_{BCS} of the head in the desired direction $\mathbf{h1}_{BCS}$ (and by this way passage frame through head). The frame's initial point of passage is $B(1)_{LCS}$ and the end point is $B(N)_{LCS}$. The REE trajectory is determined by the sequence of the TCP_i values, where $1 \le i \le N$. The initial position of REE corresponds to the value TCP_0. In the admissible REE position, the two orthogonal vectors and their common initial point originally defined in the *LCS* are in the same position in the *BCS* as the two fixed orthogonal vectors and their common initial point specified in the *BCS*. The position and orientation of the REE in *BCS* in the *i*-th step of the passing of the frame through the fibre processing head are uniquely determined by the relation (1). The identification of vectors $\mathbf{b2}(i)_{BCS}$ and $\mathbf{h2}_{BCS}$ allows the performance of the necessary rotation of the frame around the tangent of axis *o*orientation at point $B(i)_{BCS}$ when the point $B(i)_{BCS}$ is identified with centre of the head H_{BCS} (*Fig. 3*).

$$B(i)_{BCS} \equiv H_{BCS},\ \mathbf{b1}(i)_{BCS} \equiv \mathbf{h1}_{BCS} \text{ and } \mathbf{b2}(i)_{BCS} \equiv \mathbf{h2}_{BCS} \text{ for } 1 \le i \le N. \tag{1}$$

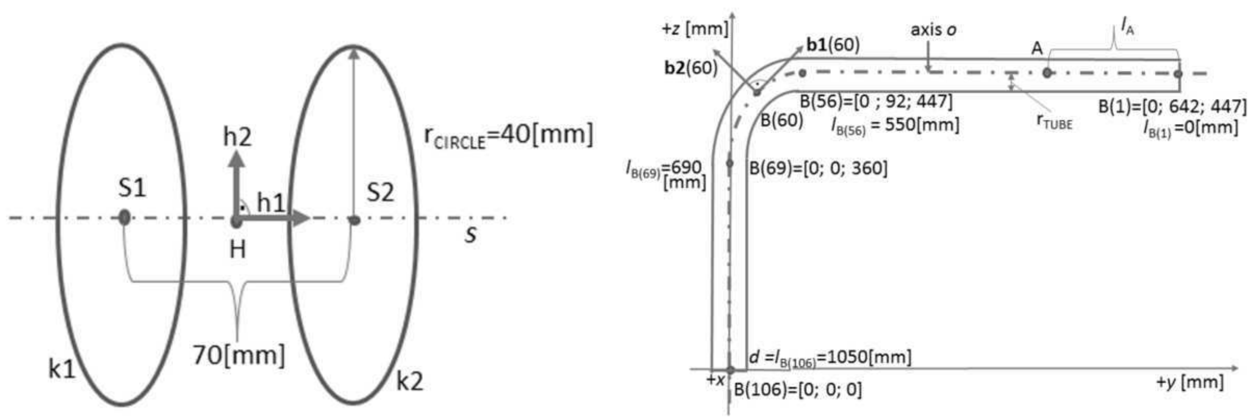

***Fig. 2** a) The fibre-processing head in the mathematical model, b) Example of vertical cross-section non-bearing frame*

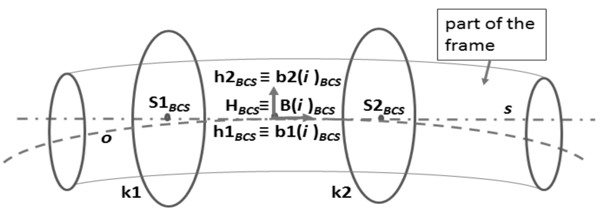

***Fig. 3** The passing frame through the fibre processing head in the i-th step*

Calculation of the TCP$_i$

Now we focus on the process determination of the TCP_i. We use matrix calculus to solve this problem. Points, vectors and matrices are represented in a homogeneous form (i.e. general point $V = [x_V, y_V, z_V, 1]^T$, vector $\mathbf{u} = (x_u, y_u, z_u, 0)^T$, this form of writing is suitable for differentiation of operations with points and vectors. We calculate transformation matrix $\mathbf{T}_i$ from *LCS* to *BCS* for the *i*-th step of passing the frame through the fibre processing head. The transformation matrix $\mathbf{T}_i$ is generally the product of the translation matrix $\mathbf{L}_i$ and the rotation matrix $\mathbf{Q}_i$, i.e.

$$\mathbf{T}_i = \mathbf{L}_i \cdot \mathbf{Q}_i \tag{2}$$

Validity of relation (1) is reached by applying matrix $\mathbf{T}_i$ in relation (2) to *LCS*.

We use the following typesorthogonal matrices: $\mathbf{Rot}(z, a)$ is orthogonal matrix of rotation of *LCS* around axis *z* by angle *a*, $\mathbf{Rot}(y, b)$ orthogonal matrix of rotation of *LCS* around axis *y* by angle *b* and $\mathbf{Rot}(x, c)$ orthogonal matrix of rotation of *LCS* around axis *z*by angle *c*. Hereat it is true (see [6])

$$\mathbf{Rot}(z,a) = \begin{pmatrix} \cos a & -\sin a & 0 & 0 \\ \sin a & \cos a & 0 & 0 \\ 0 & 0 & 1 & 0 \\ 0 & 0 & 0 & 1 \end{pmatrix},\ \mathbf{Rot}(y,b) = \begin{pmatrix} \cos b & 0 & \sin b & 0 \\ 0 & 1 & 0 & 0 \\ -\sin b & 0 & \cos b & 0 \\ 0 & 0 & 0 & 1 \end{pmatrix},\ \mathbf{Rot}(x,c) = \begin{pmatrix} 1 & 0 & 0 & 0 \\ 0 & \cos c & -\sin c & 0 \\ 0 & \sin c & \cos c & 0 \\ 0 & 0 & 0 & 1 \end{pmatrix}. \tag{3}$$

We also use matrix $\mathbf{Rot}(\mathbf{p}_{BCS}, \alpha)$ of *BCS* rotation around unit vector $\mathbf{p}_{BCS}$ by angle α that is in the form

$$\mathbf{Rot}\,(\mathbf{p}_{BCS}\,,\alpha) = \begin{pmatrix} c+n_1^2(1-c) & n_1n_2(1-c)-n_3s & n_1n_3(1-c)+n_2s & 0 \\ n_1n_2(1-c)+n_3s & c+n_2^2(1-c) & n_2n_3(1-c)-n_1s & 0 \\ n_1n_3(1-c)-n_2s & n_2n_3(1-c)+n_1s & c+n_3^2(1-c) & 0 \\ 0 & 0 & 0 & 1 \end{pmatrix},$$

wheres and c indicate $s=\sin\alpha$, $c=\cos\alpha$ .Calculation of transformation matrix $\mathbf{T}_i$ in relation (2) is described in detail in [1]. Each rotation matrix $\mathbf{Q}_i$ can be written in the form (see [6])

$$\mathbf{Q}_i = \mathbf{Rot}(z, a_i)\cdot\mathbf{Rot}\,(y, b_i)\cdot\mathbf{Rot}(x, c_i)\,, \qquad (4)$$

where matrices $\mathbf{Rot}(z, a_i)$, $\mathbf{Rot}(y, b_i)$ and $\mathbf{Rot}(x, c_i)$ are in the form in relation (3). Then Euler angles a_i, b_i and $c_i$can be expressed in the form (for more detail see [1] and [2])

$$a_i = ATAN\,2\left(q_{21}(i), q_{11}(i)\right),\; b_i = ATAN\,2\left(-q_{31}(i), q_{11}(i)\cos a_i + q_{21}(i)\sin a_i\right), \qquad (5)$$
$$c_i = ATAN2\left(q_{13}(i)\sin a_i - q_{23}(i)\cos a_i,\; q_{22}(i)\cos a_i - q_{12}\sin a_i\right).$$

The *ATAN2*(*arg1*, *arg2*) function (common in many programming languages) calculates the value of the arctangent function for the argument arg1/arg2. The signsof both input parameters are involved in determining the output angle of the *ATAN2* function ($-\pi < ATAN2(\text{arg1, arg2}) \le \pi$).Thus, we determine a_i, b_i and c_i in equation (4). Now,we can determine $TCP_i = (x_i, y_i, z_i, a_i, b_i, c_i)$, where parameters x_i , y_i and z_i are determined by matrix $\mathbf{L}_i$ in relation (2) and the last three parameters a_i, b_i and c_i are given by relation (5).

Determination of REE trajectory

By entering the calculated set of TCP_i into the robot's control unit the robot creates (by specified commands) a continuous trajectory of the REE allowing the passage of the frame through the fibre-processing head. The trajectory is created on the principle of linear interpolation (or the use of cubic splines) of the parameters included in TCP_i ($1 \le i \le N$). It is necessary to perform the calculation for a sufficient amount of points $B(i)_{LCS}$ so that the position of the frame in LCS is sufficiently accurate.

2.2 Optimization of the REE trajectory

Compliance of the correct angles of fibre winding of individual layers on the frame is one of the most important conditions for ensuring the high quality production of frame composites. Three consecutive layers of fibres are wound onto the frame at angles of 30°,45°,60°, 0° (fibres of this layer are placed horizontally in the direction of axis *s* of the fibre-processing head) and -30°,-45°,-60°. The correct winding anglesare ensured if frame axis *o* is orthogonal to the planes of the fibres winding $\rho 1$ and $\rho 2$ (Fig.4) at points M1 and M2 of the intersectionsaxis *o*with these planes.The second important requirement is that points M1and M2 lie on axis *s* or near axis *s*of the fibre-processing head. Achieving these conditions can be difficult in practice. The frame can be highly 3D shaped. Collision-free passageof the frame through the head must also be ensured. Middle horizontal fibres winding is fastened to the frame by the final third fibrewinding performed in plane $\rho 2$.

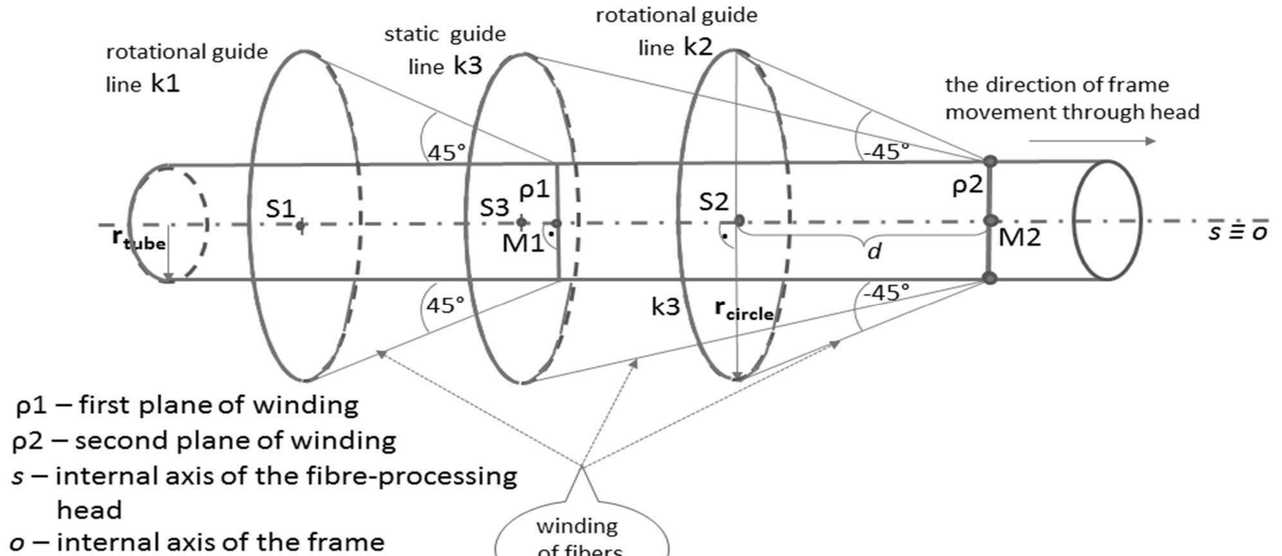

Fig. 4 *Schema of winding fibre layers onto the frame, case where the axes s and o are identical in the section of the fibre-processing head*

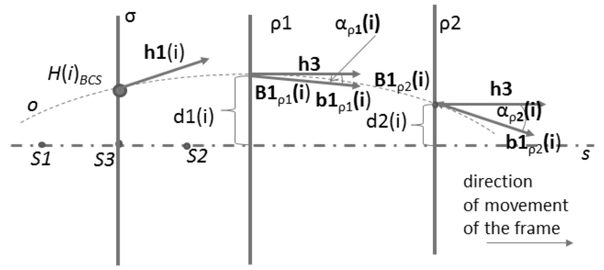

Fig. 5 Intersections of axis o with planes $\rho1$ and $\rho2$

The idea of REE trajectory optimization

Calculation of REE trajectory for *i*-th step of frame passage through the fibre-processing head in Chapter 3 was performed on the basis of fulfilling relation (1) (i.e. it is doing such rotation and translation *LCS* (of the REE) with respect to *BCS*, that $B(i)_{BCS} \equiv H_{BCS}$, $\mathbf{b1}(i)_{BCS} \equiv \mathbf{h1}_{BCS}$ and $\mathbf{b2}(i)_{BCS} \equiv \mathbf{h2}_{BCS}$ are true). Point $H_{BCS} \equiv S3_{BCS}$ (Fig. 6), vectors $\mathbf{h1}_{BCS}$ and $\mathbf{h2}_{BCS}$ are constant throughout the whole frame passage through the head. The main idea of optimizing the REE trajectory is as follows. When performing optimization, we find suitable locations of point H_{BCS} and vectors $\mathbf{h1}_{BCS}$, $\mathbf{h2}_{BCS}$ in every step of passage frame through the head that the required conditions for ensuring that the correct angles of winding are adhered to. We suppose in our mathematical model that axis *y*of system *BCS* is identical to internal axis *s* of the fibre-processing head. Point $H(i)_{BCS}$ lies in the plane σ that is orthogonal to axis *s* and that passes through the centre of head $S3_{BCS}$ (see Fig. 5, $1 \le i \le N$). We obtain vector $\mathbf{h1}(i)_{BCS}$ by rotation of vector $\mathbf{h1}_{BCS} = (0, 1, 0, 0)$ around axis z at angle $\varphi(i)$ and then around axis x at angle $\omega(i)$. The same rotations are applied to vector $\mathbf{h2}_{BCS} = (0, 0, 1, 0)$ and we obtain vector $\mathbf{h2}(i)_{BCS}$. We can write rotations of vectors $\mathbf{h1}_{BCS}$ and $\mathbf{h2}_{BCS}$ in the form

$$\mathbf{h1}(i)_{BCS} = Rot(z, \varphi(i)) \cdot Rot(x, \omega(i)) \cdot \mathbf{h1}_{BCS}\ ,\ \mathbf{h2}(i)_{BCS} = Rot(z, \varphi(i)) \cdot Rot(x, \omega(i)) \cdot \mathbf{h2}_{BCS}\ , \tag{6}$$

where $-\pi/4 \le \varphi(i) \le \pi/4$, $-\pi/4 \le \omega(i) \le \pi/4$ for $1 \le i \le N$. We can then identify analogously to relation (1):

$$B(i)_{BCS} \equiv H(i)_{BCS}\ ,\ \mathbf{b1}(i)_{BCS} \equiv \mathbf{h1}(i)_{BCS}\ ,\ \mathbf{b2}(i)_{BCS} \equiv \mathbf{h2}(i)_{BCS} \text{ for } 1 \le i \le N. \tag{7}$$

Now, we will focus on minimizingcost function *F* to finding optimized REE trajectory. Function *F* is defined in the form

$$F(x_{H(i)_{BCS}}, z_{H(i)_{BCS}}, \varphi(i), \omega(i)) = v_1\left(d1(i)^2 + v_3 \cdot \alpha_{\rho1}(i)^2\right) + v_2\left(d2(i)^2 + v_3 \cdot \alpha_{\rho2}(i)^2\right), \tag{8}$$

where values $d1(i)$, $\alpha_{\rho1}(i)$, $d2(i)$ and $\alpha_{\rho2}(i)$ (see Figure 7) depend on values of variables $x_{H(i)_{BCS}}, z_{H(i)_{BCS}}, \varphi(i)$ and $\omega(i)$ .Point $H(i)_{BCS}$ lies in plane σ and therefore coordinate $y_{H(i)_{BCS}}$ is constant (we recall that axes *s* is identical with axes *y* in *BCS*). Value *d1* denotesdistance of point $B1_{\rho1}(i)_{BCS}$ (intersection axis *o* of frame with first winding plane $\rho1$) from point $M1(i)_{BCS}$ (Fig. 7), angle $\alpha_{\rho1}(i)$ is defined by vector **h3** (parallel with axis *s*)and tangent vector of axis *o* at point $B1(i)_{BCS}$. Values *d2(i)* and $\alpha_{\rho2}$ *(i)* are defined analogously. Parameters $v_1$and v_2 denote weight functions and characterize the importance of the quality of winding layer. Parameter v_3 corrects the value ratio of $d1(i)$ and $\alpha_{\rho1}(i)$ respectively $d2(i)$ and $\alpha_{\rho2}(i)$. We find global minimum of cost function *F* in relation (8), i.e.

$$F(x(i)_{\min}, z(i)_{\min}, \varphi(i)_{\min}, \omega(i)_{\min}) = \min\left\{ F(x_{H(i)_{BCS}}, z_{H(i)_{BCS}}, \varphi(i), \omega(i)) \right\}. \tag{9}$$

We determine TCP_iusing the minimized input parameters $x(i)_{\min}$, $z(i)_{\min}$, $\varphi(i)_{\min}$, $\omega(i)_{\min}$ of cost function *F* defined by relation (9), calculation ofpoint $B(i)_{BCS}$ by relation (7) and unit vectors $\mathbf{h1}(i)_{BCS}$ and $\mathbf{h2}(i)_{BCS}$ by relation (6).

Note.

We suppose that internal axis *o* of composite frame is defined by set of points $B(i)_{LCS}$ and corresponding vectors $\mathbf{b1}(i)_{LCS}$ and $\mathbf{b2}(i)_{LCS}$ with a small step along this axis. Otherwise, we can define the small step using spline function, for example quadratic Hermite spline. We get more points $B(i)_{LCS}$ on axis *o*and corresponding unit vectors ($\mathbf{b1}(i)_{LCS}$, $\mathbf{b2}(i)_{LCS}$) by this procedure. We need the fulfillment of this condition for optimized REE trajectory calculation.

Optimization by differential evolution algorithm

Cost function *F* defined by (8) often contains many local minima. Therefore, using gradient methods for finding the global minimum of the function *F* is not suitable (the high probability, that we find only thelocal minimum). Therefore, we use a classical differential evolution algorithm usually denoted *DE/rand/1/bin* (for more detail see [13,14]). It is often difficult to find global minimum cost function defined by relation (9). But then we are able to find a satisfactory local minimum.We also apply restrictions in the search for the minimum function F so that the absolute values of differences of corresponding parameters of TCP_{i-1} and TCP_i are smaller than small positive real constant.

Optimization by differential evolution algorithm

Cost function F defined by (8) often contains many local minima. Therefore, using gradient methods for finding the global minimum of the function F is not suitable (the high probability, that we find only thelocal minimum). Therefore, we use a classical differential evolution algorithm usually denoted *DE/rand/1/bin* (for more detail see [13,14]). It is often difficult to find global minimum cost function defined by relation (9). But then we are able to find a satisfactory local minimum.We also apply restrictions in the search for the minimum function F so that the absolute values of differences of corresponding parameters of TCP_{i-1} and TCP_i are smaller than small positive real constant.

Pseudo-code of differential evolution algorithm

We briefly describe differential evolution algorithm *DE/rand/1/bin* that we used to the solution of optimization problem (9).

- **Input:**

The initial individual y_1 - initial values $x_{H(i)BCS}, z_{H(i)BCS}, \varphi(i), \omega(i)$;dimension of the problem D= 4, population size NP, crossover probability CR, mutation factor f, the number of calculated generations NG.

Internal computation:

1. create an initial generation (G =0) of NP individuals y_m^G, $1 \le m \le NP$,

2. a) evaluate all the individuals y_m^G of the generation G (calculate $F(y_m^G)$ for every individual y_m^G),

b) store the individuals y_m^G and their evaluations $F(y_m^G)$ into the matrix **B** (every matrix row contains parameters of individual y_m^G and its evaluation $F(y_m^G)$, $1 \le m \le NP$),

3. *repeat until* $G \le NG$

a) *form*:=1 *step* 1 to *NP do*

(i) randomly select index $k_m \in \{1, 2, \dots, D\}$,

(ii) randomly select indexes $r_1, r_2, r_3 \in \{1, \dots, NP\}$, where $r_l \ne m$ for $1 \le l \le 3$; $r_1 \ne r_2, r_1 \ne r_3, r_2 \ne r_3$;

(iii) *forj*:=1 step 1 to D do

if (rand(0,1) ≤ CR or j=k_m)*then*

$y_{m,j}^{trial} := y_{r_3,j}^G + f\left(y_{r_1,j}^G - y_{r_2,j}^G\right)$

else

$y_{m,j}^{trial} := y_{m,j}^G$

end for (j)

(iv) *if* $F\left(y_m^{trial}\right) \le F\left(y_m^G\right)$ *then* $y_m^{G+1} := y_m^{trial}$

else $y_m^{G+1} := y_m^G$

end for (m)

c) store individuals y_m^{G+1} and their evolutions $F\left(y_m^{G+1}\right)$ $(1 \le m \le NP)$ of the new generation G+1 into the matrix B; G:= G+1

end repeat.

- **Output:**

The row of matrix **B** that contains the corresponding value $\min\{F\left(y_m^G\right); y_m^G \in \mathbf{B}\}$ represents the best found individual y_{opt}.

Comment:

Function rand(0,1) randomly chooses a number from the interval $\langle 0,1 \rangle$. The notation $y_{m,j}^G$ means the j-th component of an individual y_m^G in the G-th generation.

The individual y_{opt} is the final solution and includes optimized parameters $x(i)_{\min}$, $z(i)_{\min}$, $\varphi(i)_{\min}$ and $\omega(i)_{\min}$ in relation (9).

3 Results

We focus on the practical problem of the passage of the non-bearing 3D frame for aerospace apllication with a non-circular cross-section through the fibre-processing head. The central 2D axis o of the frame is composed of two interconnected perpendicular arms (Fig. 1). The rotation is performed during the passage of the bent portion of the frame through the fibre-processing head. The calculation of the trajectory of the robot-end-effector by used numerical modelling referred to in the previous chapter was applied to the described problem. Fig. 6 a) shows the position of the robot-end-effector when passing 3D frame through winding head. In part b) shows trajectory of the robot-end-effector: start and end. c) shows the position of the robot-end-effector (first three parameters of TCP) and part d) the orientation of the robot-end-effector (last three parameters of TCP). Fig. 7 and Fig. 8 are comparison numerical model and real experiment illustrates the individually calculated values of TCP during the passing of the frame through fibre-processing head. Manufacturing process of real sample by data from numerical modelling is seen in the ***Fig. 9***. Optimal fiber placement from winding process with data of numerical model also results in a better connection with a matrix, because the poor fiber placement (winding process without data of numerical model) arises imperfect connection as mentioned in [2].

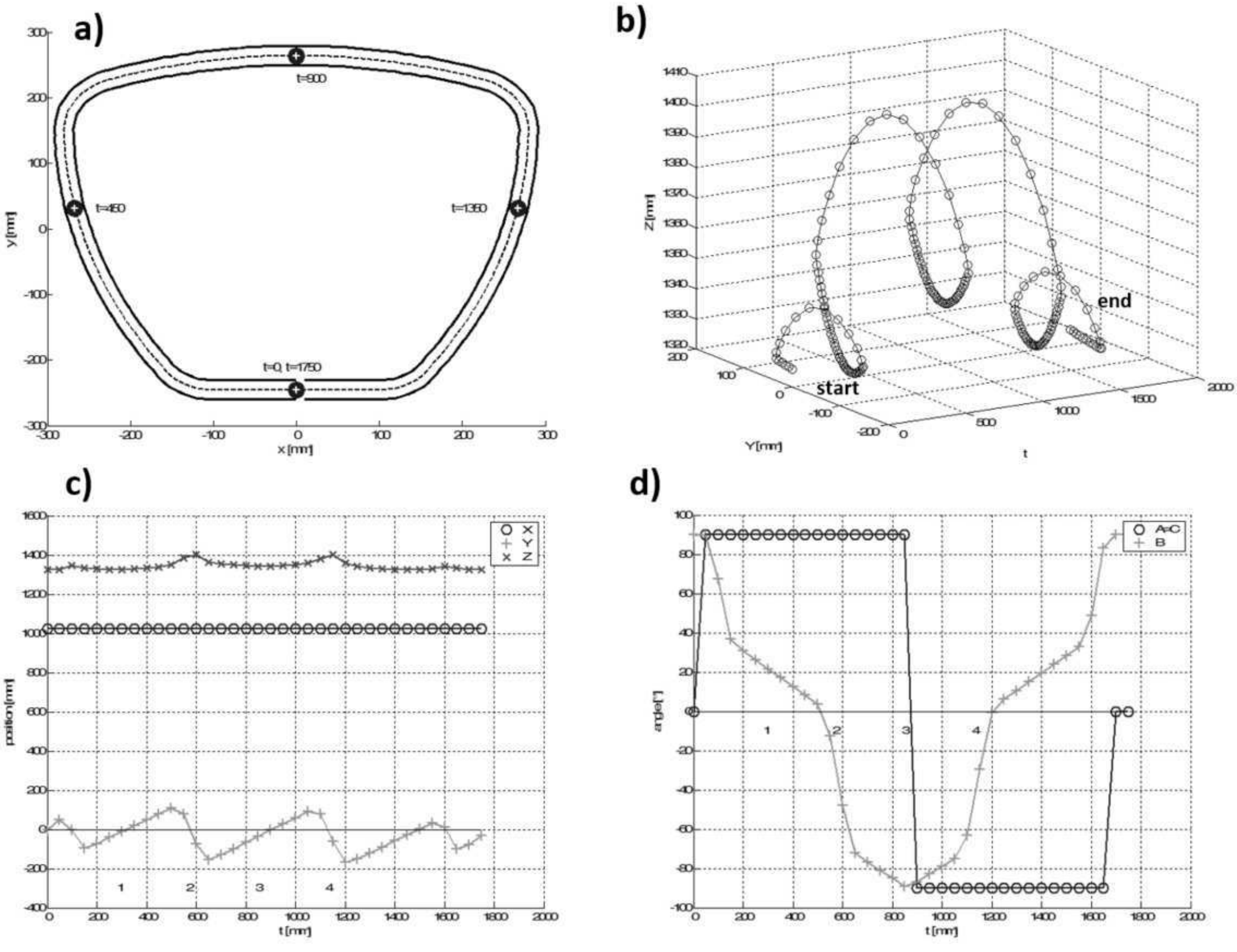

***Fig. 6** a) Diagram showing numerical modelling for optimization of the course of the TCP during the passing of the aerospace frame through the fibre-processing head, b) trajectory of the robot-end-effector: start and end, c) parameter values of the first three parameters of TCP, d) parameter values of the last three parameters of TCP*

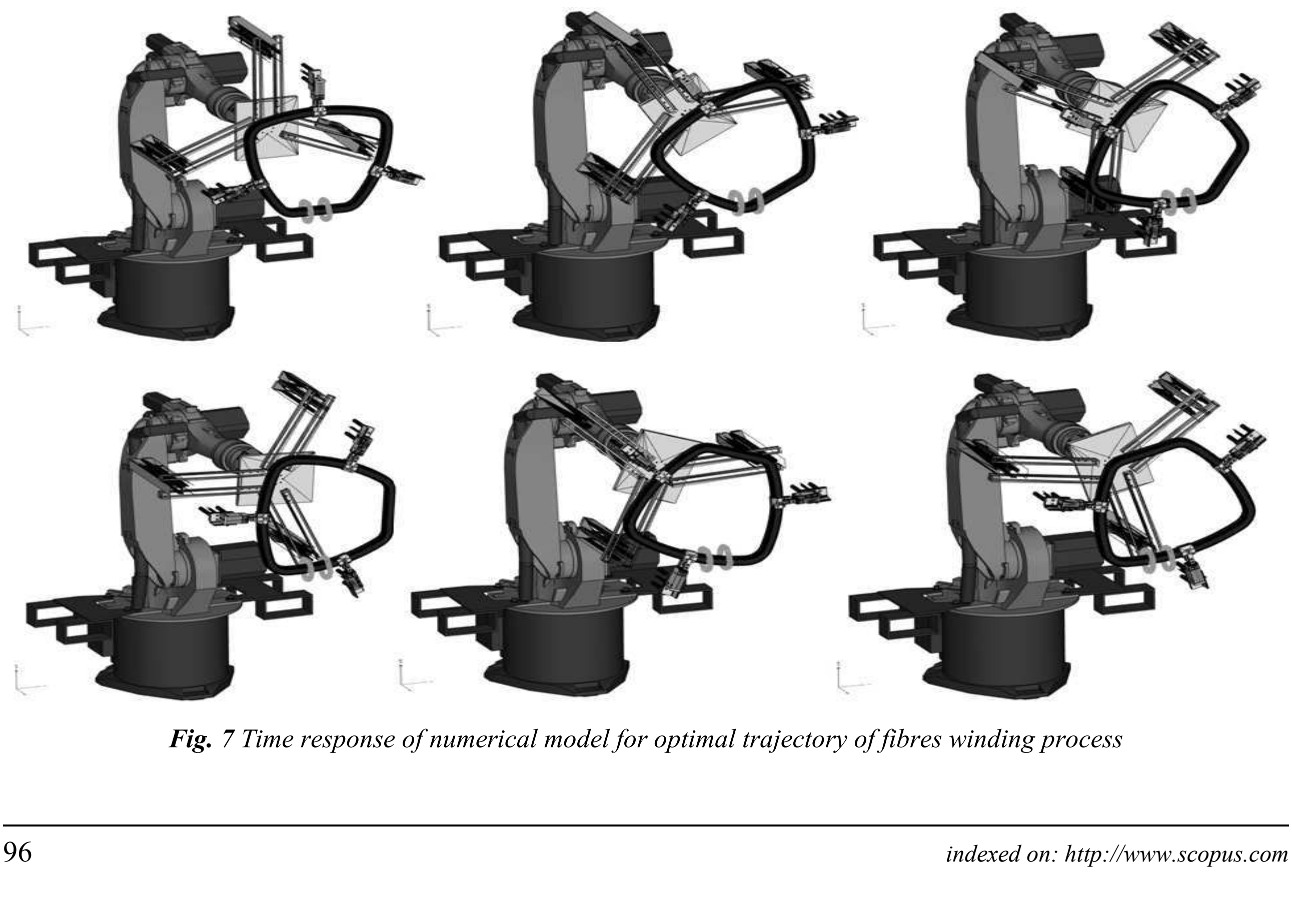

***Fig.** 7 Time response of numerical model for optimal trajectory of fibres winding process*

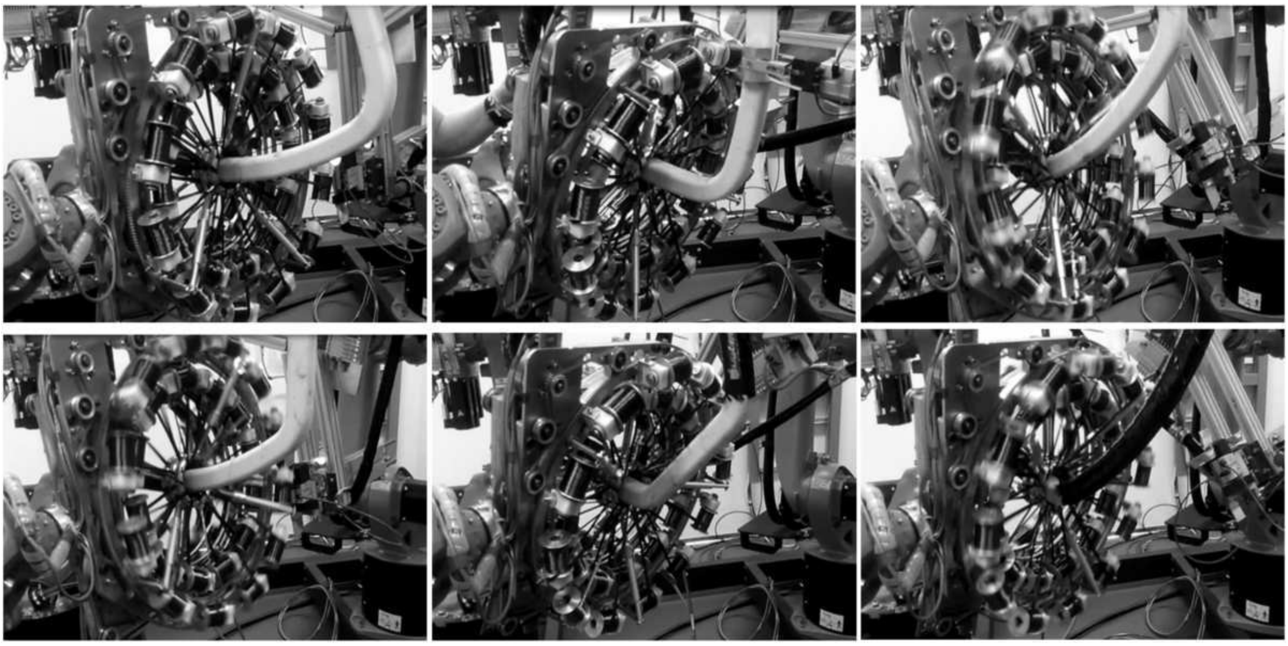

Fig. 8 *Time response of real testing of trajectory of fibres winding process with same data as numerical model*

Fig. 9 *Laboratory samples from winding process with data of numerical model*

4 Conclusion

The numerical algorithm described in the article allows calculating the 3D trajectory of the robot-end-effector of the industry robot during the production of composites using the dry fibre winding technology on a frame. Currently, supply companies offer commercial software modules to robot users. These modules are used in areas such as welding, pressing, cutting, packing and gluing. However, the available software tools are not usable for our needs. The algorithm can be applied to any manufacturing process where it is necessary to determine the 3D trajectory of a robot-end-effector. Especially, this algorithm can be successfully used in the industrial production of specific composites as are aerospace frames. The algorithm allows us to determine the exact trajectory of the robot-end-effector, which provides a significant advantage over a manually entered robot trajectory. The manual setting requires experienced technicians and is time-consuming (usually it is necessary to repeatedly enter a testing trajectory to find a satisfactory one). In addition, the trajectory obtained by such procedure is not usually optimal. The use of the described algorithm is completely independent of the type of production robot and software tools. The described mathematical algorithm can be successfully utilized by technicians of manufacturing robotic workplaces and also by developers of specific software tools for controlling the manufacture robots. Described algorithm can be also successfully used in robot trajectory optimization using mathematical methods. The procedure for determining the trajectory of the robot-end-effector induces virtually no additional costs to the manufacturer and can significantly speed up the determination of the desired trajectory of the robot-end-effector.

Acknowledgement

The results of this project No. LO1201 were obtained through the financial support of the Ministry of Education, Youth and Sports, Czech Republic in the framework of the targeted support of the "National Programme for Sustainability I".

References

[1] MARTINEC T, MLÝNEK J, PETRŮ, M. (2015). Calculation of the robot trajectory for the optimum directional orientation of fibre placement in the manufacture of composite profile frames. *Robotics and Computer-Integrated Manufacturing*, Vol. 35, pp. 42-54.

[2] PETRŮ, M., MARTINEC, T., MLÝNEK J. (2016). Numerical Model Description of Fibres Winding Process for New Technology of Winding Fibres on the Frames. In: *Manufacturing Technology*, Vol. 16, N.4, pp. 786-792.

[3] GAY, D., HOA, S. (2007). Composite materials – design and applications. *CRC press, Taylor & Francis Group*, London, ISBN: 978-1-4200-4519-2

[4] KULHAVÝ, P., LEPŠÍK, P. (2017). Digitization of Structured Composite Plates with Regard to Their Numerical Simulations. In: *Manufacturing Technology*, Vol. 17, N.2, pp. 198-203.

[5] NOVAKOVA-MARCINCINOVA, L., NOVAK-MARCINCIN, J. (2014). Production of abs-aramid composite material by fused deposition modeling rapid prototyping system. In: *Manufacturing Technology*, Vol. 14, N.1, pp. 85-91.

[6] SCIAVICCO, L., SICILIANO. B. (2004). Modelling and Control of Robot Manipulators. London: Springer, 2004, ISBN: 978-1-84628-641-4

[7] ANDULKAR , M. V. , CHIDDARWAR , S. S. (2015). Incremental approach for trajectory generation of spray painting robot, *Industrial Robot: An International Journal*, Vol. 42, Iss. 3, pp.228 - 241.

[8] BRUNETE , A., MATEO, C. , GAMBAO, E. , HERNANDO , M., KOSKINEN , J.,AHOLA, J. M. ,SEPPALA , T., HEIKKILA , T. (2016). User-friendly task level programming based on an online walk-through teaching approach, *Industrial Robot: An International Journal*, Vol. 43, IsS. 2, pp.153 – 163.

[9] SWOLFS, Y., CRAUVELS, L., BREDA, V., B., GORBATIKH, L., HLINE, P., WARD, I. VERPOEST, I. (2014).Tensile behaviour of intralayer hybrid composites of carbon fibre and self-reinforced polypropylene", Composites Part A, vol. 59 (2014) pp. 78-84. DOI:10.1016/j.compositesa.2014.01.001

[10] HUANG, Z., M., ZHOU, Y., X. (2012), Strength of Unidirectional Composites, Advanced Topics in Science and Technology in China, pp.99–143.

[11] MASSA , D., CALLEGARI , M., CRISTINA, C. (2015). Manual guidance for industrial robot programming, *Industrial Robot: An International Journal*, Vol. 42, Iss. 5, pp.457 – 465.

[12] XIAO, Y., DU, Z., DONG, W. (2012). Smooth and near time optimal trajectory planning of industrial robots for online applications, *Industrial Robot: An International Journal*, Vol. 39, Iss. 2, pp.169 – 177.

[13] PRICE, K., V., STORN, R., M., LAMPIEN, J., A. (2005). Differential Evolution. Springer-Verlag, Berlin, Heidelberg

[14] KNOBLOCH, R., MLYNEK, J., SRB, R. (2017). The Classic Differential Evolution Algorithm and Its Covergence Properties, *J. Application of Mathematics*, 62, No. 2, Institute of Mathematics of the Czech Academy of Sciences, Prague, pp. 197-208.

DOI: 10.21062/ujep/59.2018/a/1213-2489/MT/18/1/90